

**HIGH-THROUGHPUT SCREENING ASSAY IN  
384-WELL FORMAT FOR THE  
IDENTIFICATION OF ANTI-TRYPANOSOMAL  
AGENTS AGAINST *TRYPANOSOMA BRUCEI*  
*RHODESIENSE* AND MODE OF CELL DEATH  
STUDY**

**LIM KAH TEE**

**UNIVERSITI SAINS MALAYSIA**

**2017**

**HIGH-THROUGHPUT SCREENING ASSAY  
IN 384-WELL FORMAT FOR THE  
IDENTIFICATION OF ANTI-TRYPANOSOMAL  
AGENTS AGAINST *TRYPANOSOMA BRUCEI*  
*RHODESIENSE* AND MODE OF  
CELL DEATH STUDY**

by

**LIM KAH TEE**

**Thesis submitted in fulfillment of the requirements  
for the degree of  
Doctor of Philosophy**

**February 2017**

## ACKNOWLEDGEMENT

I am indebted to many individuals who helped me throughout my study. First of all it is an honour for me to express my deep sense of gratitude to my supervisor, Prof. Dr. Mohd. Ilham bin Adenan, and co-supervisor, Assoc. Prof. Dr. Zafarina binti Zainuddin, for their valuable guidance and support from the initial to the final level that enabled me to develop an understanding of the project. I am grateful to those who made this thesis possible and an enjoyable experience for me, especially to my friends for the encouragement to pursue this study and technical assistance. I also owe my sincere gratitude to my family for generous support, inspiration, emotional understanding, fidelity and unconditional love. I am very much thankful to Swiss Tropical and Public Health Institute (Swiss TPH), Basel for providing the strain of *Trypanosoma brucei rhodesiense* STIB 900 and standard drug melarsoprol used throughout this study. I acknowledge with thanks the financial support (E-Science Fund: 02-05-20-SF0005) provided by the Ministry of Science, Technology and Innovation (MOSTI) of Malaysia in conducting this study at Malaysian Institute of Pharmaceuticals and Nutraceuticals (IPharm). I also gratefully acknowledge the MyBrain15 scholarship received towards my Ph.D. from the Ministry of Higher Education Malaysia (MOHE). Lastly, I offer my regards and blessings to all of those who supported me in any aspect during the completion of this study.

## TABLE OF CONTENTS

<b>ACKNOWLEDGEMENT</b> .....	ii
<b>TABLE OF CONTENTS</b> .....	iii
<b>LIST OF TABLES</b> .....	viii
<b>LIST OF FIGURES</b> .....	x
<b>LIST OF SYMBOLS AND ABBREVIATIONS</b> .....	xv
<b>LIST OF APPENDICES</b> .....	xviii
<b>LIST OF EQUATIONS</b> .....	xx
<b>ABSTRAK</b> .....	xxi
<b>ABSTRACT</b> .....	xxiii
<b>CHAPTER 1: INTRODUCTION</b> .....	1
1.1 Problem statements.....	3
1.2 Justification for the study.....	4
1.3 Aims of the study.....	5
<b>CHAPTER 2: LITERATURE REVIEW</b> .....	6
2.1 <i>Trypanosoma brucei</i> .....	6
2.1.1 Classification.....	8
2.1.2 Morphology of African trypanosomes.....	8
2.1.3 Life cycle of <i>T. brucei</i> .....	11
2.2 Human African trypanosomiasis.....	14
2.2.1 Diagnosis of HAT.....	18
2.2.2 Treatment of HAT.....	19
2.3 High-throughput screening in anti-trypanosomal drug discovery.....	22
2.3.1 HTS assays formats: 96-, 384- and 1536-well formats.....	24
2.4 Anti-trypanosomal activity of plant natural products.....	26
2.5 <i>Senna spectabilis</i> (DC.) H.S.Irwin & Barneby.....	27
2.5.1 Classification.....	28
2.5.2 Ethnomedicinal uses.....	30
2.5.3 Bioactive constituents and pharmacological properties.....	30

2.6	Programmed cell death of African trypanosomes.....	34
2.6.1	Apoptosis.....	36
2.6.2	Autophagy.....	38
2.6.3	Necrosis and paraptosis.....	41
2.7	Detection of programmed cell death.....	41
	<b>CHAPTER 3: MATERIALS AND METHODS.....</b>	<b>43</b>
3.1	Materials and apparatuses.....	44
3.1.1	Chemicals, reagents and media.....	44
3.1.2	Consumables.....	45
3.1.3	Equipments.....	46
3.2	Media and solutions preparation.....	47
3.2.1	Basal minimum essential medium for <i>T. b. rhodesiense</i> and assays..	47
3.2.2	Minimum essential media.....	48
3.2.3	Baltz supplement.....	48
3.2.4	2-mercaptoethanol solution.....	49
3.2.5	Dulbecco's modified eagle medium for rat skeletal (L6) myoblast cell line and assays.....	49
3.3	Preparation of detection reagents.....	49
3.3.1	Resazurin.....	49
3.3.2	Vanillin/sulphuric acid.....	50
3.3.3	Dragendorff.....	50
3.3.4	MitoTracker <sup>®</sup> Red CMXRos.....	51
3.3.5	CellEvent <sup>™</sup> Caspase-3/7 Green.....	51
3.3.6	Monodansylcadaverine.....	52
3.4	Preparation of stock solutions of standard drugs.....	52
3.4.1	Preparation of stock solutions of pentamidine and melarsoprol for trypanosome assay.....	52
3.4.2	Preparation of stock solutions of podophyllotoxin for cytotoxicity assay.....	52
3.5	Trypanosome cultures.....	53
3.5.1	Maintenance of <i>T. b. rhodesiense</i> .....	53

3.5.2	Thawing of cryostabilates.....	53
3.5.3	Basic culture of <i>T. b. rhodesiense</i> .....	54
3.5.4	Preparation of cryostabilates of <i>T. b. rhodesiense</i> .....	54
3.6	Cell line culture.....	55
3.6.1	Maintenance of rat skeletal (L6) myoblast cell line.....	55
3.6.2	Thawing cryostabilates.....	55
3.6.3	Basic culture of L6 cell line.....	56
3.6.4	Preparation of cryostabilates of L6 cell line.....	56
3.7	Development of anti-trypanosomal assay in 384-well format for high-throughput whole cell viability screening assay of <i>T. b. rhodesiense</i> .....	57
3.7.1	Cell counting.....	57
3.7.2	Maximum trypanosome density and doubling time of <i>T. b. rhodesiense</i> in T-25 culture flask.....	61
3.7.3	Optimization of <i>T. b. rhodesiense</i> viability and resazurin fluorescence signal.....	61
3.7.4	Optimization of seeding trypanosome density.....	65
3.7.5	Effect of DMSO on trypanosome viability.....	67
3.7.6	Linearity and sensitivity of the HTS assay.....	70
3.7.7	Determination of the half maximal inhibitory concentration of reference drugs.....	70
3.7.8	Reference drugs sensitivity assay.....	73
3.7.9	Optimized HTS assay.....	73
3.8	Evaluation of the <i>in vitro</i> anti-trypanosomal activity of 1,333 plant extracts by a whole cell viability based HTS campaign.....	74
3.8.1	Plant collections.....	75
3.8.2	Preparation of stock solutions of plant extracts for HTS campaign.....	75
3.8.3	Primary screening.....	78
3.8.4	Secondary screening: retest primary screening hits.....	82
3.8.5	L6 cytotoxicity assay.....	85
3.9	Bioassay-guided isolation of compound <b>1</b> and <b>2</b> from the leaves of <i>S. spectabilis</i> against <i>T. b. rhodesiense</i> .....	88
3.9.1	Plant material.....	88

3.9.2	Extraction.....	88
3.9.3	Solvent partitioning.....	89
3.9.4	Isolation and purification.....	89
3.9.5	Structure elucidation.....	90
3.9.6	Bioassays for extracts, fractions and compounds.....	91
3.10	Mode of cell death study of <i>T. b. rhodesiense</i> induced by (+)-spectaline and iso-6-spectaline.....	93
3.10.1	Analysis by SEM and TEM.....	93
3.10.2	Measurement of mitochondrial membrane potential.....	94
3.10.3	Detection of PS exposure.....	94
3.10.4	DNA fragmentation analysis.....	95
3.10.5	Determination of caspase-like protease activity.....	96
3.10.6	Autophagy assay.....	96
3.11	Statistical analysis.....	97
	<b>CHAPTER 4: RESULTS.....</b>	<b>99</b>
4.1	Development of anti-trypanosomal assay in 384-well format for high-throughput whole cell viability screening assay of <i>T. b. rhodesiense</i> .....	99
4.1.1	Maximum trypanosome density and doubling time of <i>T. b. rhodesiense</i> in T-25 culture flask.....	99
4.1.2	Optimization of <i>T. b. rhodesiense</i> viability and resazurin fluorescence signal.....	99
4.1.3	Optimization of seeding trypanosome density.....	106
4.1.4	Effect of DMSO on trypanosome viability.....	112
4.1.5	Linearity and sensitivity of the HTS assay.....	114
4.1.6	Reference drugs sensitivity assay.....	118
4.2	Evaluation of the <i>in vitro</i> anti-trypanosomal activity of 1,333 plant extracts by HTS campaign.....	121
4.3	Bioassay-guided isolation of compound <b>1</b> and <b>2</b> from leaves of <i>S. spectabilis</i> against <i>T. b. rhodesiense</i> .....	128
4.3.1	Structure elucidation of compound <b>1</b> .....	136
4.3.2	Structure elucidation of compound <b>2</b> .....	147

4.4	Cell death actions study of <i>T. b. rhodesiense</i> induced by (+)-spectaline and iso-6-spectaline.....	158
4.4.1	Analysis by SEM and TEM.....	158
4.4.2	Measurement of mitochondrial membrane potential.....	170
4.4.3	Detection of PS exposure.....	172
4.4.4	DNA fragmentation analysis.....	174
4.4.5	Determination of caspase-like protease activity.....	176
4.4.6	Autophagy assay.....	178
<b>CHAPTER 5: DISCUSSION.....</b>		<b>180</b>
<b>CHAPTER 6: CONCLUSIONS.....</b>		<b>206</b>
<b>FUTURE DIRECTIONS.....</b>		<b>208</b>
<b>REFERENCES.....</b>		<b>209</b>
<b>APPENDICES.....</b>		<b>223</b>
<b>LIST OF PUBLICATIONS</b>		



## LIST OF TABLES

		<b>Page</b>
Table 2.1	Summary of drug therapy in HAT.	21
Table 2.2	Summary of bioactive constituents isolated from various parts of <i>S. spectabilis</i> and its pharmacological activities.	33
Table 2.3	Some common features of PCD observed in trypanosomatids.	33
Table 3.1	List of chemicals, reagents and media used in this study.	44
Table 3.2	List of consumables used in this study.	45
Table 3.3	List of laboratory equipments used in this study.	46
Table 3.4	Preparation of BMEM.	47
Table 3.5	Preparation of MEM.	48
Table 3.6	Preparation of Baltz supplements.	48
Table 3.7	Preparation of 2-mercaptoethanol solution.	49
Table 3.8	Preparation of DMEM.	49
Table 3.9	Preparation of resazurin reagent.	50
Table 3.10	Preparation of vanillin/sulphuric acid reagent.	50
Table 3.11	Preparation of Dragendorff reagent.	51
Table 3.12	Various concentrations of resazurin added to each volume of trypanosomes to make a final concentration of 10% resazurin in the 384-well plate.	64
Table 3.13	Ten microliters of various concentrations of DMSO added into each well containing 40 $\mu$ L of cells to make a final concentration of 0.1 to 3.0% DMSO.	69
Table 4.1	Estimation of 50% inhibitory concentration ( $IC_{50}$ ) $\pm$ SD values using fluorescence signals and cell counts of reference drugs in the two variant HTS assay 384-well formats.	119
Table 4.2	Number of plant samples active against <i>T. b. rhodesiense</i> in the primary screening.	123

Table 4.3	Anti-trypanosomal activity, cytotoxic effects and selectivity indices of plant samples active against <i>T. b. rhodesiense</i> in the secondary screening.	125
Table 4.4	Physical characteristics, anti-trypanosomal activity, cytotoxic effect, and selectivity indices of the extracts, fractions and compounds from the leaves of <i>S. spectabilis</i> .	130
Table 4.5	1D and 2D NMR spectra data of compound <b>1</b> at 500 and 125 MHz for $^1\text{H}$ and $^{13}\text{C}$ , respectively, in $\text{CDCl}_3$ .	145
Table 4.6	1D and 2D NMR spectra data of compound <b>2</b> at 500 and 125 MHz for $^1\text{H}$ and $^{13}\text{C}$ , respectively, in $\text{CDCl}_3$ .	156
Table 5.1	Estimation of $\text{IC}_{50}$ with the resazurin-based 96-well assay formats found in the literature for <i>T. b. rhodesiense</i> .	187
Table 5.2	Examples of FDA-approved drugs with origins in HTS hits.	190
Table 5.3	$^1\text{H}$ NMR spectral data for spectaline and iso-6-spectaline found in literature.	196
Table 5.4	$^{13}\text{C}$ NMR spectral data for spectaline and iso-6-spectaline found in literature.	197

## LIST OF FIGURES

		<b>Page</b>
Figure 2.1	Schematic drawing of the ultrastructure of <i>T. brucei</i> .	10
Figure 2.2	Life cycle of <i>T. brucei</i> .	13
Figure 2.3	Distribution of HAT with incidences and risk for travelers.	17
Figure 2.4	Chemical structure of registered drugs used in the treatment of HAT.	21
Figure 2.5	Comparison of 96-, 384- and 1536-well plate formats.	25
Figure 2.6	<i>S. spectabilis</i> tree.	29
Figure 3.1	Research methodology flow chart.	43
Figure 3.2	Haemocytometer arrangement and dimensions.	59
Figure 3.3	Haemocytometer with Neubauer ruling.	59
Figure 3.4	Counting system in a Neubauer chamber big square.	60
Figure 3.5	Plate layout for the optimization of <i>T. b. rhodesiense</i> viability and resazurin fluorescence signal.	63
Figure 3.6	Plate layout for the optimization of seeding trypanosome density.	66
Figure 3.7	Plate layout for the investigation of effect of DMSO on trypanosome viability.	68
Figure 3.8	Plate layout for determining reference drugs IC <sub>50</sub> .	72
Figure 3.9	Flow chart of whole cell viability based HTS campaign for the identification of Malaysian plant forest species active against <i>T. b. rhodesiense</i> .	76
Figure 3.10	Locations of the plant samplings throughout reserved forest in Peninsula Malaysia and number of plant samples collected.	77
Figure 3.11	Plate layout for preparation of seventy samples to be tested in 96-well plate at concentration of 20.83 µg/mL.	80
Figure 3.12	Plate layout for preparation of seventy samples to be tested in 96-well plate at concentration of 2.6 µg/mL.	80
Figure 3.13	Plate layout for primary screening of plant samples.	81

Figure 3.14	Plate layout for secondary screening of extracts identified from primary screening.	84
Figure 3.15	Plate layout for L6 cytotoxicity assay.	87
Figure 4.1	Growth curve of <i>T. b. rhodesiense</i> in a 25 cm <sup>2</sup> culture flask over 144 h.	101
Figure 4.2	Signal detection for different concentrations of trypanosomes inoculated at various volumes in (A) clear 384-well plate and (B) black 384-well plate after 8 h incubation with 10 µL of resazurin.	102
Figure 4.3	Fluorescence development for 50 uL of <i>T. b. rhodesiense</i> at 1-, 2- and 3 × 10 <sup>6</sup> cells/mL in (A) clear 384-well plate and (B) black 384-well plate after 8 h incubation with different volumes of resazurin.	103
Figure 4.4	Fluorescence measurement for 50 uL of 3 × 10 <sup>6</sup> cells/mL <i>T. b. rhodesiense</i> in (A) clear 384-well plate and (B) black 384-well plate at different volumes of resazurin at different times.	104
Figure 4.5	Linearity for high trypanosome densities at 8 h incubation with 10 µL of resazurin.	105
Figure 4.6	Cell counts of 50 µL of varying inocula after growth for 72 h in clear- and black-384-well plate.	108
Figure 4.7	A slightly decreased in trypanosome growth to 4.04 × 10 <sup>6</sup> and 4.1 × 10 <sup>6</sup> cells/mL in clear- and black-384-well plate, respectively was detected 2 h after end read point of assay.	108
Figure 4.8	Growth curve of different initial inoculums of <i>T. b. rhodesiense</i> in 384-well plate.	109
Figure 4.9	Fluorescence measurement of 50 µL of varying inocula incubated with 10 µL of resazurin for 4 h in clear- and black-384-well plate.	110
Figure 4.10	Cell counts at varying inocula at 72 h growth at different time of incubation in the presence of resazurin.	111
Figure 4.11	Evaluation of DMSO tolerance in <i>T. b. rhodesiense</i> .	113
Figure 4.12	Fluorescence measurement of 50 µL of varying inocula incubated with 10 µL of resazurin at (i) 68 h of cell growth, followed by 4 h incubation in the presence of resazurin, and (ii) 64 h of cell growth, followed by 8 h incubation in the presence of resazurin in (A) clear 384-well plate and (B) black 384-well plate.	115

Figure 4.13	Cell counts at varying inocula at 72 h growth at different time of incubation in the presence of resazurin with (i) 68 h of cell growth, followed by 4 h incubation in the presence of resazurin, and (ii) 64 h of cell growth, followed by 8 h incubation in the presence of resazurin.	116
Figure 4.14	Linearity for $1 \times 10^3$ to $3 \times 10^4$ cells/mL inoculums at 68 h of cell growth, followed by 4 h of growth in the presence of 10 $\mu$ L of resazurin.	117
Figure 4.15	Dose-response of reference drugs on <i>T. b. rhodesiense</i> growth following 72 h incubation in the presence of (A) pentamidine and (B) melarsoprol.	120
Figure 4.16	Number of plant samples that were active against <i>T. b. rhodesiense</i> in the primary screening.	124
Figure 4.17	Number of plant samples that were active against <i>T. b. rhodesiense</i> in the secondary screening.	124
Figure 4.18	Voucher herbarium specimen of <i>S. spectabilis</i> (PID 070412-01).	126
Figure 4.19	Voucher herbarium specimen of <i>T. grandiflora</i> (PID 070412-02).	127
Figure 4.20	TLC profile of the four organic extracts partitioned from crude MeOH extract using the solvent system Hex/EtOAc/MeOH 7:2:1.	131
Figure 4.21	TLC profile of the four fractions obtained from fractionation of DCM extract using the solvent system DCM/MeOH 9:1.	131
Figure 4.22	TLC profile of 100 subfractions chromatographed from F3 using the solvent system DCM/MeOH 9:1.	132
Figure 4.23	TLC profile of 180 subfractions chromatographed from F4 using the solvent system DCM/MeOH 9:1.	133
Figure 4.24	TLC of compound <b>1</b> and <b>2</b> sprayed with vanillin/H <sub>2</sub> SO <sub>4</sub> (left) and Dragendorff reagent (right).	134
Figure 4.25	Flow chart of bioassay-guided isolation of compound <b>1</b> and <b>2</b> together with their anti-trypansomal activity, cytotoxic effect and selectivity indices.	135
Figure 4.26	MS of <b>1</b> ( $m/z$ 326.40 [M + H] <sup>+</sup> ).	138
Figure 4.27	IR spectrum of <b>1</b> .	139

Figure 4.28	500 MHz $^1\text{H}$ NMR spectrum of <b>1</b> in $\text{CDCl}_3$ at 25°C.	140
Figure 4.29	500 MHz $^1\text{H}$ NMR spectrum (expansion $\delta$ 1.0 – 4.0) of <b>1</b> in $\text{CDCl}_3$ at 25°C.	141
Figure 4.30	125 MHz $^{13}\text{C}$ NMR spectrum of <b>1</b> in $\text{CDCl}_3$ at 25°C.	142
Figure 4.31	125 MHz $^{13}\text{C}$ NMR spectrum (expansion $\delta$ 10 – 80) of <b>1</b> in $\text{CDCl}_3$ at 25°C.	143
Figure 4.32	125 MHz $^{13}\text{C}$ NMR spectrum (expansion $\delta$ 28.0 – 31.0) of <b>1</b> in $\text{CDCl}_3$ at 25°C.	144
Figure 4.33	COSY and HMBC correlations of compound <b>1</b> .	146
Figure 4.34	MS of <b>2</b> ( $m/z$ 326.40 $[\text{M} + \text{H}]^+$ ).	149
Figure 4.35	IR spectrum of <b>2</b> .	150
Figure 4.36	500 MHz $^1\text{H}$ NMR spectrum of <b>2</b> in $\text{CDCl}_3$ at 25°C.	151
Figure 4.37	500 MHz $^1\text{H}$ NMR spectrum (expansion $\delta$ 1.0 – 4.0) of <b>2</b> in $\text{CDCl}_3$ at 25°C.	152
Figure 4.38	125 MHz $^{13}\text{C}$ NMR spectrum of <b>2</b> in $\text{CDCl}_3$ at 25°C.	153
Figure 4.39	125 MHz $^{13}\text{C}$ NMR spectrum (expansion $\delta$ 15 – 80) of <b>2</b> in $\text{CDCl}_3$ at 25°C.	154
Figure 4.40	125 MHz $^{13}\text{C}$ NMR spectrum (expansion $\delta$ 28.6 – 31.0) of <b>2</b> in $\text{CDCl}_3$ at 25°C.	155
Figure 4.41	COSY and HMBC correlations of compound <b>2</b> .	157
Figure 4.42	Observation by field-emmission SEM of untreated <i>T. b. rhodesiense</i> showing an elongated body and intact and smooth plasma membrane.	159
Figure 4.43	Observation by FESEM of <i>T. b. rhodesiense</i> treated with $\text{IC}_{50}$ of <b>1</b> .	160
Figure 4.44	Observation by FESEM of <i>T. b. rhodesiense</i> treated with $\text{IC}_{90}$ of <b>1</b> .	161
Figure 4.45	Observation by FESEM of <i>T. b. rhodesiense</i> treated with $\text{IC}_{50}$ of <b>2</b> .	162
Figure 4.46	Observation by FESEM of <i>T. b. rhodesiense</i> treated with $\text{IC}_{90}$ of <b>2</b> .	163

Figure 4.47	Energy-filtering TEM of untreated <i>T. b. rhodesiense</i> showing organelles with normal morphology.	165
Figure 4.48	EFTEM of <i>T. b. rhodesiense</i> treated with IC <sub>50</sub> of <b>1</b> .	166
Figure 4.49	EFTEM of <i>T. b. rhodesiense</i> treated with IC <sub>90</sub> of <b>1</b> .	167
Figure 4.50	EFTEM of <i>T. b. rhodesiense</i> treated with IC <sub>50</sub> of <b>2</b> .	168
Figure 4.51	EFTEM of <i>T. b. rhodesiense</i> treated with IC <sub>90</sub> of <b>2</b> .	169
Figure 4.52	Quantitative analysis of mitochondrial membrane potential of <i>T. b. rhodesiense</i> .	171
Figure 4.53	FACS analysis for PS exposure, measured by double staining with annexin V and PI in <i>T. b. rhodesiense</i> .	173
Figure 4.54	Analysis of DNA fragmentation in <b>1</b> - and <b>2</b> -treated <i>T. b. rhodesiense</i> for 72 h.	175
Figure 4.55	Quantitative analysis caspase-like activity in <i>T. b. rhodesiense</i> .	177
Figure 4.56	MDC labeling quantification of <b>1</b> - and <b>2</b> -treated <i>T. b. rhodesiense</i> .	179
Figure 5.1	Chemical structure of piperine isolated from <i>Piper</i> sp.	199
Figure 5.2	Schematic illustrating the stages in drug discovery.	205

## LIST OF SYMBOLS AND ABBREVIATIONS

–	negative or minus or to
%	percentage
&	and
:	ratio
~	approximately
+	positive or plus
<	less than
=	equal to
>	greater than
±	plus-minus
×	times
$\Delta\Psi_m$	mitochondrial membrane potential
≤	less-than or equal to
≥	greater-than or equal to
→	to
↔	between
®	registered
°C	degree Celcius
μg/mL	microgram per milliliter
a.u.	arbitrary unit
μL	microliter
μM	micromolar
μm	micrometer
PCR	polymerase chain reaction
ANOVA	analysis of variance
ATR	attenuated total reflection
BBB	blood-brain barrier
BMEM	basal minimum essential medium
BSC	biological safety cabinet
BuOH	butanol
Ca <sup>2+</sup>	calcium
CD <sub>3</sub> OD	methanol-d <sub>4</sub>
CDCl <sub>3</sub>	chloroform- <i>d</i>
CHCl <sub>3</sub>	chloroform
cm	centimeter
CNS	central nervous system
CO <sub>2</sub>	carbon dioxide
COSY	correlation spectroscopy
CV	coefficient of variation
DCM	dichloromethane
DCVC	dry column vacuum chromatography
DEPT	distortionless enhancement by polarization transfer



dH <sub>2</sub> O	distilled water
DMSO	dimethyl sulfoxide
DNA	deoxyribonucleic acid
e.g.	for example
EDTA	ethylenediaminetetraacetic acid
EM	electron microscope
ESI-MS	electrospray ionization mass spectrometry
EtBr	ethidium bromide
EtOAc	ethyl acetate
EtOH	ethanol
FACS	fluorescence-activated cell sorting
FBS	fetal bovine serum
FDA	Food and Drug Administration
FITC	fluorescein isothiocyanate
g	gram
h	hour
H <sub>2</sub> SO <sub>4</sub>	sulphuric acid
HAT	Human African trypanosomiasis
HEPES	4-(2-hydroxyethyl)-1-piperazineethansulfonic acid
Hex	hexane
HIV/AIDS	human immunodeficiency virus/acquired immunodeficiency syndrome
HMBC	heteronuclear multiple-bond correlation
HMQC	heteronuclear multiple-quantum correlation
HTS	high-throughput screening
i.e.	that is
IC <sub>50</sub>	half maximal inhibitory concentration
IC <sub>90</sub>	90% inhibitory concentration
kg	kilogram
KI	potassium iodide
L	liter
log	logarithm
MDC	monodansylcadaverine
MEM	minimum essential medium
MeOH	methanol
mg	milligram
mg/mL	milligram per milliliter
MHz	megahertz
min	minute
mL	milliliter
mM	millimolar
mm <sup>2</sup>	square millimeter
NaHCO <sub>3</sub>	sodium bicarbonate
NaOH	sodium hydroxide

nm	nanometer
NMR	nuclear magnetic resonance
NOESY	nuclear overhauser effect spectroscopy
OsO <sub>4</sub>	osmium tetroxide
PBS	phosphate buffer saline
PCD	programmed cell death
PCR	polymerase chain reaction
PI	propidium iodide
ppm	parts per million
PS	phosphatidylserine
rpm	revolutions per minute
S/B	signal-to-background ratio
SD	standard deviation
SDS	sodium dodecyl sulfate
SEM	scanning electron microscope
SI	selectivity index
sp.	species (singular form)
spp.	species (plural form)
TAE	Tris-acetate-EDTA
TEM	transmission electron microscope
TLC	thin layer chromatography
TMS	tetramethylsilane
Tris-HCl	Tris-hydrochloride
™	trade mark
UV	ultraviolet
UHPLC	ultra-high performance liquid chromatography
LC-MS	liquid chromatography-mass spectrometry
V	volt
v/v	volume per volume
<i>m/z</i>	mass-to-charge ratio
w/v	weight per volume
Z'	Z'-factor
δ	chemical shifts
1D	one-dimensional
<sup>1</sup> H	proton NMR
1N	one normality
2D	two-dimensional
<sup>13</sup> C	carbon NMR

## LIST OF APPENDICES

		<b>Page</b>
Appendix 1	Chromatographic method for isolation of compound <b>1</b> from DCM extract-DCVC-F3.	224
Appendix 2	Chromatographic method for isolation of compound <b>2</b> from DCM extract-DCVC-F4.	225
Appendix 3	SEM processing protocol for cells from EM Unit, USM.	226
Appendix 4	TEM processing protocol for tissues from EM Unit, USM.	227
Appendix 5	Experimental protocol for measurement of mitochondrial membrane potential using MitoTracker Red CMXRos from Invitrogen (Cat. no. M7512).	228
Appendix 6	Recommended procedure for detection of PS exposure using annexin V-FITC counterstained with PI from Invitrogen (Cat. no. 33-1200).	229
Appendix 7	DNA ladder detection protocol for DNA fragmentation analysis from Invitrogen (Cat. no. GTX85527).	230
Appendix 8	Experimental protocol for determination of caspase-like protease activity using Caspase-3/7 Green detection reagent from Invitrogen (Cat. no. C10423).	231
Appendix 9	125 MHz <sup>13</sup> C NMR and DEPT spectrum (expansion $\delta$ 5 – 80) of <b>1</b> in CDCl <sub>3</sub> 25°C.	232
Appendix 10	HMQC spectrum of <b>1</b> in CDCl <sub>3</sub> at 25°C.	233
Appendix 11	HMQC spectrum of <b>1</b> (expansion $\delta$ 0.5 – 4.0) in CDCl <sub>3</sub> at 25°C.	234
Appendix 12	HMQC spectrum of <b>1</b> (expansion $\delta$ 0.8 – 2.3) in CDCl <sub>3</sub> at 25°C.	235
Appendix 13	HMQC spectrum of <b>1</b> (expansion $\delta$ 3.2 – 3.8) in CDCl <sub>3</sub> at 25°C.	236
Appendix 14	COSY spectrum of <b>1</b> in CDCl <sub>3</sub> at 25°C.	237
Appendix 15	COSY spectrum of <b>1</b> (expansion $\delta$ 1.5 – 4.5) in CDCl <sub>3</sub> at 25°C.	238
Appendix 16	COSY spectrum of <b>1</b> (expansion $\delta$ 0.7 – 2.6) in CDCl <sub>3</sub> at 25°C.	239

Appendix 17	HMBC spectrum of <b>1</b> in CDCl <sub>3</sub> at 25°C.	240
Appendix 18	HMBC spectrum (expansion $\delta$ 1.2 – 2.8) of <b>1</b> in CDCl <sub>3</sub> at 25°C.	241
Appendix 19	125 MHz <sup>13</sup> C NMR and DEPT spectrum (expansion $\delta$ 5 – 80) of <b>2</b> in CDCl <sub>3</sub> at 25°C.	242
Appendix 20	HMQC spectrum of <b>2</b> in CDCl <sub>3</sub> at 25°C.	243
Appendix 21	HMQC spectrum (expansion $\delta$ 0.5 – 4.5) of <b>2</b> in CDCl <sub>3</sub> at 25°C.	244
Appendix 22	HMQC spectrum (expansion $\delta$ 1.0 – 2.6) of <b>2</b> in CDCl <sub>3</sub> at 25°C.	245
Appendix 23	COSY spectrum of <b>2</b> in CDCl <sub>3</sub> at 25°C.	246
Appendix 24	COSY spectrum of <b>2</b> (expansion $\delta$ 1.0 – 5.0) in CDCl <sub>3</sub> at 25°C.	247
Appendix 25	COSY spectrum of <b>2</b> (expansion $\delta$ 1.0 – 2.6) in CDCl <sub>3</sub> at 25°C.	248
Appendix 26	HMBC spectrum of <b>2</b> in CDCl <sub>3</sub> at 25°C.	249
Appendix 27	HMBC spectrum (expansion $\delta$ 1.0 – 4.0) of <b>2</b> in CDCl <sub>3</sub> at 25°C.	250
Appendix 28	NOESY spectrum of <b>2</b> in CDCl <sub>3</sub> at 25°C.	251
Appendix 29	NOESY spectrum (expansion $\delta$ 0.5 – 4.5) of <b>2</b> in CDCl <sub>3</sub> at 25°C.	252
Appendix 30	Representative confocal image of MitoTracker Red labeling of <i>T. b. rhodesiense</i> following treatment with compound <b>1</b> .	253
Appendix 31	Representative confocal image of annexin V/propidium iodide binding of <i>T. b. rhodesiense</i> following treatment with compound <b>1</b> .	254
Appendix 32	Representative confocal image of caspase-3/7 binding of <i>T. b. rhodesiense</i> following treatment with compound <b>1</b> .	255
Appendix 33	Representative confocal image of MDC labeling of <i>T. b. rhodesiense</i> following treatment with compound <b>1</b> .	256
Appendix 34	Estimations of cost for high-throughput whole cell screening of <i>T. b. rhodesiense</i> in 96- and 384-well formats.	257

## LIST OF EQUATIONS

		<b>Page</b>
Equation 1	Cell concentration	58
Equation 2	Cell doubling time	61
Equation 3	Retardation factor ( $R_f$ )	90
Equation 4	Signal-to-background (S/B) ratio	97
Equation 5	Percentage of coefficient of variation (% CV)	97
Equation 6	Z'-factor	97
Equation 7	Percentage of cell inhibition	97
Equation 8	Selectivity index (SI)	98

**ASAI PENABIRAN CELUSAN TINGGI DALAM FORMAT 384-TELAGA  
UNTUK PENGENALPASTIAN EJEN ANTI-TRIPANOSOMAL TERHADAP  
*TRYPANOSOMA BRUCEI RHODESIENSE* DAN  
MOD PENGAJIAN KEMATIAN SEL**

**ABSTRAK**

Dalam usaha untuk mempercepat penemuan ubat bagi rawatan Tripanosomiasis Afrika Manusia (“*Human African Trypanosomiasis*”, HAT), adalah menjadi keperluan untuk mempunyai satu asai yang mudah dan sensitif dalam mengenalpasti “*hits*” positif berasaskan penabiran celusan tinggi (“*high-throughput screening*”, HTS) seluruh sel. Dalam kajian ini, asai HTS telah dibangunkan dalam format 384-telaga dengan membandingkan penggunaan plat cerah dan plat hitam. Keteguhan dan kebolehulangan asai yang ditentukan dalam keadaan optimum bagi plat 384-telaga adalah bersesuaian untuk asai HTS termasuk peratusan pekali variasi 4.68% dan 4.74%, nisbah isyarat-kepada-latar belakang 12.75 dan 12.07 dan faktor Z’ 0.79 dan 0.82 bagi plat telaga 384 cerah dan hitam, masing-masing. Kepekatan akhir 0.30% dimetil sulfoxide adalah optimum dalam cerakin HTS bagi kedua-dua jenis plat. Tiada perbezaan aktiviti yang signifikan dilihat apabila menggunakan ubat rujukan pentamidine dan melarsoprol bagi kedua-dua jenis plat. Oleh itu, plat cerah 384-telaga adalah sesuai untuk digunakan dalam kaedah HTS untuk mengenalpasti sebatian yang baharu terhadap *Trypanosoma brucei rhodesiense*. Sebanyak 1,333 tumbuh-tumbuhan yang dikutip dari hutan di Malaysia telah diuji dan didapati sejumlah enam pokok mempunyai potensi aktiviti anti-tripanosomal. Ekstrak tumbuhan tersebut mempunyai nilai IC<sub>50</sub> kurang daripada 1.56 µg/mL dengan indeks pemilihan (“*selectivity index*”, SI) melebihi 100. Ujian selanjutnya terhadap *T. b.*

*rhodesiense* membawa kepada pemilihan *Senna spectabilis* (IP 117; nama tempatan: Kasia Kuning) untuk pengasingan sebatian aktif secara bioasai-berpandu terhadap spesies penyebab HAT ini. Dua alkaloid piperidin yang dikenalpasti sebagai (+)-spectaline (**1**) dan iso-6-spectaline (**2**) telah diasingkan daripada daun *S. spectabilis* yang masing-masing mempunyai nilai  $IC_{50}$  0.41 dan 0.71  $\mu$ M tanpa kesan toksik pada sel L6 dengan nilai SI 134.92 dan 123.74. Sebatian **1** dan **2** boleh dianggap sebagai calon yang berpotensi untuk penemuan awal ubat bagi HAT. Lanjutan daripada itu, perubahan dalam ultrastruktur tripanosom yang disebabkan oleh kedua-dua sebatian tersebut yang membawa kepada kematian sel teraturcara (“*programmed cell death*”, PCD) telah dikenalpasti dengan menggunakan mikroskop elektron. Perubahan ini termasuk jumlah pembahagian sel tripanosom yang luar biasa, kedutan pada permukaan tripanosom, kinetoplas yang tidak teratur, pembengkakan mitokondria dan pembentukan autofagosom. Penemuan ini membuktikan bahawa kematian sel secara autofagik mungkin berlaku dalam *T. b. rhodesiense*. Tambahan pula, pembentukan vakuol autofagik dan kerosakan mitokondria seperti dilihat dalam mikroskop elektron telah dibuktikan melalui pelabelan *monodansylcadaverine* dan *MitoTracker Red*. Menariknya, tripanosom yang dirawat dengan sebatian **1** dan **2** pada kepekatan tinggi ( $IC_{90}$ ) selepas 72 jam menunjukkan sebatian tersebut juga menyebabkan PCD apoptosis awal, termasuk pendedahan fosfatidilserina, kehilangan potensi membran mitokondria dan pengaktifan *caspases*. Mengambil kira semua ini secara bersama, penemuan ini juga menunjukkan potensi sebatian **1** dan **2** sebagai kemoterapi semula jadi yang mungkin mewujudkan komunikasi silang di antara autofagi dan apoptosis dalam *T. b. rhodesiense*. Kajian ini melaporkan buat kali pertama penemuan kesan penghambat, aspek ultrastruktur dan selular sebatian ini terhadap *T. b. rhodesiense*.

**HIGH-THROUGHPUT SCREENING ASSAY IN 384-WELL FORMAT FOR  
THE IDENTIFICATION OF ANTI-TRYPANOSOMAL AGENTS AGAINST  
*TRYPANOSOMA BRUCEI RHODESIENSE* AND  
MODE OF CELL DEATH STUDY**

**ABSTRACT**

In order to accelerate the discovery of novel leads for the treatment of Human African Trypanosomiasis (HAT), it is necessary to have a simple and sensitive assay to identify positive hits by whole cell viability based high-throughput screening (HTS). In this study, the HTS assay was developed in 384-well format using clear plate and black plate, for comparison. Assay robustness and reproducibility were determined under the optimized conditions in 384-well plate was well tolerated in the HTS assay, including percentage of coefficient of variation of 4.68% and 4.74%, signal-to-background ratio of 12.75 and 12.07, and  $Z'$  factor of 0.79 and 0.82 in clear- and black-384-well plate, respectively. Final concentration of 0.30% dimethyl sulfoxide was well tolerated in the HTS assay in both types of plate. No significant differences were observed for reference drugs pentamidine and melarsoprol used in the two plate format. Therefore, clear 384-well plate was suitable for use in the HTS campaign for the identification of new compounds against *Trypanosoma brucei rhodesiense*. A total of 1,333 plants collected from Malaysian forest were tested using the HTS system developed and six plants were found to have potent anti-trypanosomal activity. These plants extract have an  $IC_{50}$  value less than 1.56  $\mu\text{g/mL}$  with associated selectivity indices (SI) greater than 100. Further testing against *T. b. rhodesiense* led to the selection of *Senna spectabilis* (IP 117; local name: “Kasia Kuning”) for further bioassay-guided isolation against the causative species of HAT.



Two known piperidine alkaloids (+)-spectaline (**1**) and iso-6-spectaline (**2**) were isolated from the leaves of *S. spectabilis* with the greatest IC<sub>50</sub> values of 0.41 and 0.71 μM. Compound **1** and **2** showed no toxic effect on L6 cells with associated SI of 134.92 and 123.74, respectively which can be considered potential candidates for HAT early drug discovery. Subsequently, the ultrastructural alterations in the trypanosome induced by these compounds leading to programmed cell death (PCD) were characterized using electron microscopy. These alterations include unusual amount of trypanosome at dividing state, wrinkling of the trypanosome surface, alterations in the kinetoplast, swelling of the mitochondria, and the formation of autophagosomes. These findings evidence a possible autophagic cell death in *T. b. rhodesiense*. Furthermore, the formation of autophagic vacuoles and mitochondrial damages through monodansylcadaverine and MitoTracker Red labeling agrees with the electron microscopy data. Interestingly, trypanosomes treated with high concentration (IC<sub>90</sub>) of compound **1** and **2** after 72 h exhibited significantly induces an early apoptosis-like PCD, which includes phosphatidylserine exposure, loss of mitochondrial membrane potential and caspases activation. Taken together, these findings demonstrated the potential of compound **1** and **2** as a natural chemotherapeutic capable of inducing a possible cross-talk between autophagy and apoptosis in *T. b. rhodesiense*. This is the first report on the inhibitory effect, ultrastructural and cellular aspects of these two piperidine alkaloids on *T. b. rhodesiense*.

## CHAPTER 1

### INTRODUCTION

Human African Trypanosomiasis (HAT) also known as “sleeping sickness” is caused by two protozoan parasites, *Trypanosoma brucei rhodesiense* and *Trypanosoma brucei gambiense*. The trypanosomes are transmitted to human by a bite of the infected *Glossina* spp. (tsetse fly) and multiply extracellular in blood, lymph and cerebrospinal fluid. The disease affects about 50 millions of people yearly in 36 sub-Saharan Africa with an estimated incidence of about 30,000 cases per annum (Bowling *et al.*, 2012). The disease has two distinct stages. In the early stage, trypanosomes reproduce in hemolymphatic system of the patient whereas in the second stage, trypanosomes cross the blood-brain barrier (BBB) to the central nervous system (CNS) that results in a coma and finally death of the patient if left untreated. Endemics prevalent in rural regions where public health facilities needed for an effective treatment are absent. At present, there are only few drugs registered for the treatment of HAT, such as suramin, pentamidine, melarsoprol, eflornithine, and nifurtimox. Except for eflornithine and nifurtimox, the other drugs were developed half century ago (Phillips *et al.*, 2013; Steverding, 2010). Suramin and pentamidine are effective against the early stage of HAT whereas the second stage of the disease can only be treated with melarsoprol and eflornithine. Drugs for the treatment of sleeping sickness are depending on the causative subspecies and their ability to cross the BBB. In addition, antigenic variation that protects the trypanosome to survive attack by the host’s immune response poses difficulties in developing vaccines for the treatment of the disease (Bacchi, 2009).

For saving humanity from the neglected diseases, Drugs for Neglected Diseases *initiative* (DNDi) was founded in 2003 by four publicly-funded research institutes from Malaysia, India, Kenya, and Brazil, along with the Institut Pasteur and Médecins Sans Frontières (MSF). The organization is a not-for-profit research and development organization that develops effective, safe and inexpensive medicines for neglected diseases that trouble millions people in the poorest countries. DNDi focuses on developing new treatments for the most neglected patients suffering from diseases such as sleeping sickness, leishmaniasis, chagas disease, paediatric HIV, filarial disease, mycetoma, hepatitis C, and malaria. Tackling the burden of neglected diseases is not an easy task for any one organization alone. Malaysia being a mega-diverse country hosts an enormous diversity of plant. A large number of plants found in Malaysian rainforests have not yet been studied for their pharmaceutical potentials against the parasite. Thus, a special research group was established aims to investigate the pharmaceutical properties of Malaysian plants for their potential for the treatment of HAT, one of the most neglected life threatening diseases. In an effort to improve the drawback of current treatment of HAT, plant secondary metabolites could be a source of new drugs with strong activity and low cytotoxicity effect (Alviano *et al.*, 2012). Specifically in the last decade, phytotherapy has received great attention in the search for alternatives to chemotherapy in parasitic control (Meulas-Serrano *et al.*, 2000). The use of natural products in the treatment of various diseases can be traced back in folk medicines. Plants and their derived secondary metabolites are an attractive source of lead compounds because they have numerous bioactive molecules which may be effective against protozoa. Over the last decade, several natural compounds including alkaloids, phenolics, glycosides, and

terpenes have been identified to have inhibitory effects on the growth of kinetoplastid protozoa (Gehrig and Efferth, 2008).

In the HAT early drug discovery, resazurin-based viability assay was adopted for medium-throughput screening of small extract libraries against *T. brucei* spp. in 96-well format (Zahari *et al.*, 2014; Ioset *et al.*, 2009; Raz *et al.*, 1997). With the technological advancements in liquid handling robotics, luciferase- (Mackey *et al.*, 2006) and resazurin-based (Bowling *et al.*, 2012) whole cell viability assay have also been used extensively in 96-well format for high-throughout screening (HTS) of large set of chemical libraries against *T. b. brucei*. However, due to the intensive labor requirements and costly, this 96-well method is inappropriate for undertaking HTS of larger libraries. Therefore, to accelerate the early discovery of novel leads for the treatment of HAT, HTS of diverse extracts or compound collections for the detection of positive hits by whole cell screening in 384-well format should be undertaken. It was hypothesized that the anti-trypanosomal assay in 384-well format for HTS whole cell viability screening of *T. b. rhodesiense* would fulfill HTS criteria.

### **1.1 Problem statements**

Since trypanosomes have been recognized as human pathogens, HAT has been considered as one of the most devastating health and economic development problems in sub-Saharan Africa. Current treatment for HAT are very limited and not ideal due to toxicity and impractical administration regimes, a situation that poses significant challenges in poorly equipped areas with inadequate medical facilities and resources. No other treatments available if the strains of trypanosome have evolved resistance to the limited drugs currently used in chemotherapy (Gehrig and Efferth, 2008). Besides that, except for eflornithine, the mechanisms of action of current

drugs still remain poorly understood. Many pharmaceutical companies are unwilling to develop drugs for HAT because developing an effective drug needs high costs and capital, and knowing that their aim markets are the poorer countries – Asia, Latin America and Sub-Saharan Africa (Martyn *et al.*, 2007). All of these factors highlight the need to screen and discover new drug leads with high activity and low toxicity effect against HAT for future drug development.

## **1.2 Justification for the study**

Ninety six-well method is inappropriate for undertaking HTS of large libraries because of labor intensive, expensive and time consuming. To accelerate the detection of novel leads for the treatment of HAT, the development of a whole cell viability assay using human-infective forms of *Trypanosoma* in 384-well format would be very helpful for early drug discovery. Whole cell *in vitro* HTS screening is currently in use to find out novel trypanocidal compounds. However, these HTS assays are most often done with one particular non-human pathogenic strain (*T. b. brucei* strain 427). Less often a hit is established *in vivo* and *in vitro* on the human trypanosome parasites (Reet *et al.*, 2013). Therefore, there is a need to develop an HTS assay for detection of viability of human causative agent trypanosome: *T. b. rhodesiense* in 384-well format. The developed HTS assay system would be applicable in the discovery of potential HAT drugs and searching for potential trypanocidal compounds against the parasite. *T. b. rhodesiense* was used in screening for initial identification of anti-trypanosomal agents because it was also found to be more susceptible to standard drugs than other *T. brucei* subspecies.

In an attempt to overcome the problems of current treatment of HAT, plant and their derived products could be an interesting source of lead compounds with strong

activity and low cytotoxicity effect. Several studies have demonstrated the anti-trypanosomal activity of plant natural products. The toxicity and possible anti-trypanosomal properties of the plants collected from Malaysia forest shall be evaluated through *in vitro* approach for the identification of anti-trypanosomal agents. Elucidation of molecular events of programmed cell death (PCD) in *T. b. rhodesiense* may lead to the discovery of new targets for future chemotherapeutic drug development.

### **1.3 Aims of the study**

In order to accelerate the discovery of novel leads for the treatment of HAT, it is essential to have a simple, robust and inexpensive HTS assay to identify bioactive compounds from plant resources targeting *T. b. rhodesiense*. Therefore, the specific objectives of this study include:

1. To develop anti-trypanosomal assay in 384-well format for high-throughput whole cell viability screening of *T. b. rhodesiense*,
2. To evaluate the *in vitro* anti-trypanosomal activity of 1,333 plant extracts by a whole cell viability based HTS campaign,
3. To conduct bioassay-guided isolation of bioactive compounds from selected active plants against *T. b. rhodesiense*, and
4. To study the cell death actions of *T. b. rhodesiense* induced by the bioactive compounds.

## CHAPTER 2

### LITERATURE REVIEW

#### 2.1 *Trypanosoma brucei*

*Trypanosoma* is a genus of kinetoplastids, a group of unicellular parasitic flagellate protozoa. The name is derived from the Greek word *trypano* which means “borer” and *soma* means “body” owing to their corkscrew-like movement. The scientific name was given in 1899 after the discovery of the parasite by Sir David Bruce in 1894 (Steверding, 2008). *Trypanosoma brucei* is a protozoan parasite that causes African trypanosomiasis, or mostly known as “nagana” in animals and “sleeping sickness” in humans. The main reservoir host for *T. b. brucei* and *T. b. rhodesiense* is cattle or wild bovid, while humans serve as the main reservoir host for *T. b. gambiense*. However, transmission of the disease between animal and animal, animal and human, and human and human all take place with *T. b. rhodesiense* (Keating *et al.*, 2015).

The taxonomic relationships of the three *T. brucei* have been identified using various molecular techniques such as isoenzyme analysis, restriction fragment length polymorphism (RFLP) and mini satellite marker analysis (Njiru *et al.*, 2004), enable them to be grouped into three subspecies: *brucei*, *gambiense* and *rhodesiense*. The first one is not infective to humans even though it is genotypically resembles to the other two pathogenic subspecies because of its vulnerability to lysis by trypanosome lytic factor-1 (TLF-1) i.e., apolipoprotein L-1 (ApoL-1) molecule, a naturally-occurring toxins in primates serum that give protection against infection by several African trypanosomiasis; while the latter two are typically parasites of humans because both appear to be resistance to this serum constituent (Stephensa *et al.*, 2012;

Kiefta *et al.*, 2010). Throughout history, African trypanosomiasis has badly oppressed the economic and cause losses of US\$ 1.5 bilion in agricultural profits every year (Faria *et al.*, 2014), where it reduces livestock productivity by up to 50% (Ibrahim *et al.*, 2014).

Most *T. brucei* are heteroxenous and transmitted through an insect vector (*Glossina* spp.) in the insect's blood meal. They survive and reproduce extracellular in the hemolymphatic system of their mammalian hosts. As they move between insect and mammal in their life cycle, the parasites undergo a series of morphological changes. The life cycles of *T. brucei* spp. is initiated in human skin infected with metacyclic forms. The trypanosomes then transform to bloodstream forms and spread through draining lymph node into the circulatory system (Sternberg, 2004). In addition, the bloodstream forms *T. brucei* are well-known for their variant surface glycoprotein (VSG) coats, capable of drawing out both independent B-cell and T-cell dependent responses of host adaptive immune system, and cause chronic disease by undergoing antigenic variation (Sternberg, 2004). African trypanosome is one of several parasites that can cross the BBB (Masocha and Kristensson, 2014). Hence, there is an urgent need for the development of new HAT drugs that is active against the late stage of the disease.



### 2.1.1 Classification

The taxonomic classification of *T. brucei* is as follows (Baral, 2010):

Kingdom	: Excavata
Phylum	: Euglenozoa
Class	: Kinetoplastida
Order	: Trypanosomatida
Family	: Trypanosomatidae
Subfamily	: Trypanozoon
Genus	: <i>Trypanosoma</i>
Species	: <i>brucei</i>
Subspecies	: <i>brucei</i>
	<i>gambiense</i>
	<i>rhodesiense</i>

### 2.1.2 Morphology of African trypanosomes

*T. brucei* is an unicellular eukaryotic cell of 20 – 30 µm in length (Baral, 2010). It has elongated and tapered body shape. Trypanosomes contain all major organelles like other eukaryote cells, for example the nucleus, mitochondrion, endoplasmic reticulum (ER), Golgi apparatus, and flagellum (Souza, 2008; Overath and Engstler, 2004). Along with these common structures, the protozoan kinetoplasts are characterized by possession of several unique morphological features such as the kinetoplast, subpellicular microtubule array and the paraflagellar rod (Figure 2.1). The kinetoplast which contains DNA is an integral part of the mitochondrial system closely associated with the flagellar basal body (Overath and Engstler, 2004; Parsons *et al.*, 2001). The extraordinary molecular configuration of the deoxyribonucleic acid (DNA) contained in the kinetoplast was only discovered in the early 1970s (Souza,

2008). It is situated near the base of the flagellum and is linked to the flagellum basal body by a cytoskeletal structure. The cytoskeleton of kinetoplastids is mainly made up of highly polarized microtubules in a highly sub-pellicular array, which runs parallel in the inner face of the plasma membrane along the long axis of the cell. This defines the cell shape and ensures the cell is intact throughout the cell cycle (Matthews, 2005). These microtubules are also resistant to low temperature and several drugs used to disrupt the microtubules such as colchicines, colcemid and Taxol (Souza, 2008). The first electron microscopic studies revealed the paraflagellar rod (lattice structure of proteins) specific to the kinetoplastida presence in the flagellum of trypanosomatids due to its localization (Souza, 2008). The flagellum originates close to the flagellar pocket and the kinetoplast, and for a large part is attached to the main cell body by an undulating membrane. The flagellum consists of flagellar axoneme which positions parallel to the paraflagellar rod. The typical microtubule axoneme position in the 9+2 arrangement, oriented with the “+” at the anterior end and the “-” in the basal body. The primary role of the flagellum is locomotion and attachment to the insect vector gut in the procyclic phase. Flagellar motility is essential for the bloodstream trypanosome viability (Broadhead *et al.*, 2006). The mouth of the flagellar pocket is the most posterior part of the trypanosome. This is the exit end for the flagellum. The flagellar pocket is the only location of exo- and endo-cytosis (Overath and Engstler, 2004). This is very important in bloodstream forms because the cell membrane is coated with VSG that is synthesized in the Golgi apparatus and transported from the ER to the surface (Matthews, 2005). VSG coat protects them from the mammalian host adaptive and innate immune response. When the trypanosomes changes into procyclic forms in the insect vector midgut the VSG is replaced by a similarly thick coat of procyclins.

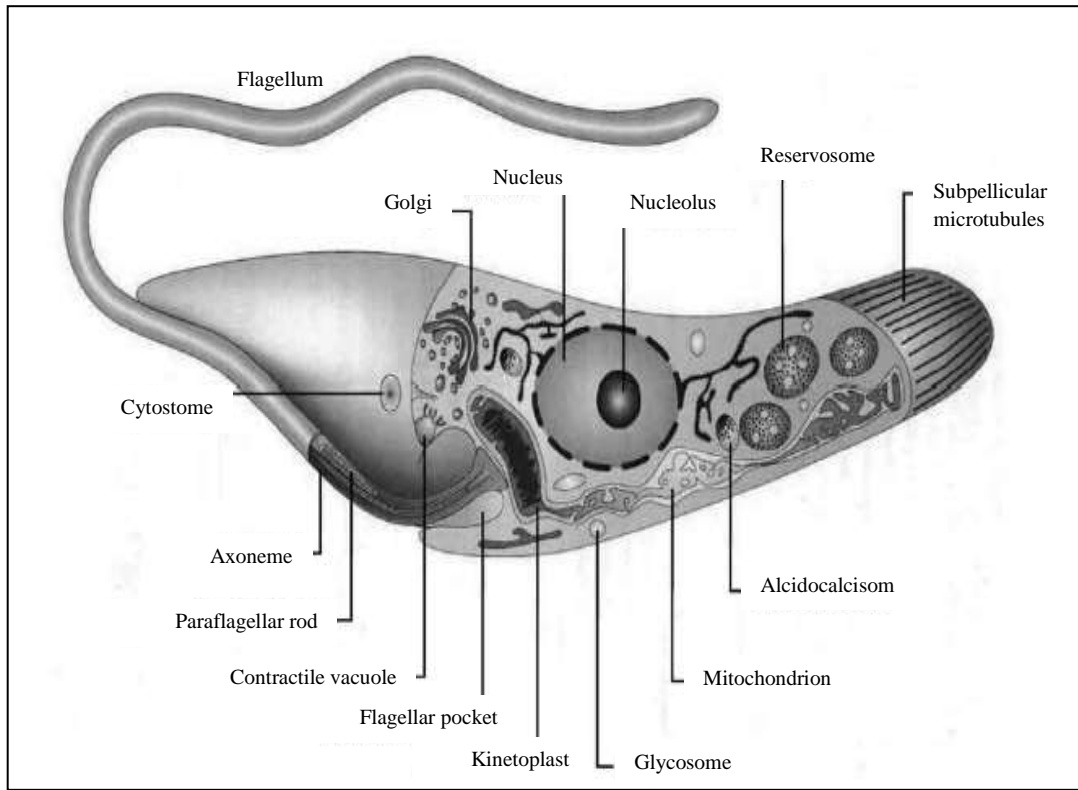


Figure 2.1: Schematic drawing of the ultrastructure of *T. brucei*. Adapted from Souza (2008).

### 2.1.3 Life cycle of *T. brucei*

*T. brucei* group trypanosomes are obliged to complete their life cycle between *Glossina* spp. (tsetse fly) and mammalian hosts such as humans, cattles and wild animals. During the differentiation at each stage of the life cycle, trypanosomes frequently change their morphology, metabolism and the major surface proteins. Figure 2.2 summarizes the life cycle of *T. brucei*. The infection begins when metacyclic trypanosomes in the saliva of the tsetse fly are injected into skin tissue of a mammal during the insect's blood meal. In some infections, chancre (a local inflammatory response to the trypanosomes), happens at the place of inoculation and subsides after 4 weeks (Naessens *et al.*, 2003). In the host, metacyclic trypanosomes transform into bloodstream trypomastigotes (proliferative long-slender form) and spread via the draining lymphatic nodes into the bloodstream. The long-slender trypomastigotes are also able to cross the placenta (Brun *et al.*, 2010). The long-slender forms (dividing form) replicate by binary fission until large numbers build up in the blood. The dividing form of trypanosomes transform first into intermediate forms and finally short-stumpy forms (non-dividing form) that are infective to tsetse fly. These stumpy form trypanosomes stay alive for only two to three days if they are not ingested by a tsetse fly in a blood meal as the trypanosomes produce prostaglandin D<sub>2</sub> (PGD<sub>2</sub>) which will lead to PCD (Figarella *et al.*, 2005). Bloodstream form trypomastigotes are covered by a VSG coat, which protects them to survive on the mammalian host's immune response (Immunoglobulin M and G) that will neutralizes the trypanosomes (Wenzler *et al.*, 2016).

When biting on an infected mammalian host, the tsetse fly is infected with bloodstream trypomastigotes. In the tsetse fly midgut, the short-stumpy trypanosomes differentiate into procyclic forms (pre-adapted for transmission to the

fly). When bloodstream trypomastigotes differentiate into procyclic forms, they shed their VSG coat and replace it by a procyclin coat (Wenzler *et al.*, 2016). The procyclic forms multiply by binary fission and cross the peritrophic membrane to arrive at the proventriculus and become mesocyclic forms and later epimastigote forms. Sexual reproduction can happen in salivary glands although it is not obligatory in trypanosomes. Sexual reproduction enables quick transmission of vital characteristics such as virulence and drug resistance, and genetic exchange (Franco *et al.*, 2014). The epimastigotes travel through the esophagus, proboscis, and hypopharynx to the salivary gland where they attached to the epithelium of salivary gland and differentiate into infectious metacyclic forms (Franco *et al.*, 2014). During the insect's blood meal they are injected into the mammalian host along with the saliva. Genetic exchange is common in *T. b. rhodesiense*, but it is infrequent in *T. b. gambiense* (Koffi *et al.*, 2007). The cycle in the fly takes about 21 days. For most of its life cycle in the tse-tse fly vector, the trypanosomes do not need a VSG coat. The metacyclic form trypanosomes is the only stage that is infective to mammalian host, and it is identified by the presence of the VSG coat that will help the trypanosomes to survive in the host (Wenzler *et al.*, 2016; Franco *et al.*, 2014).

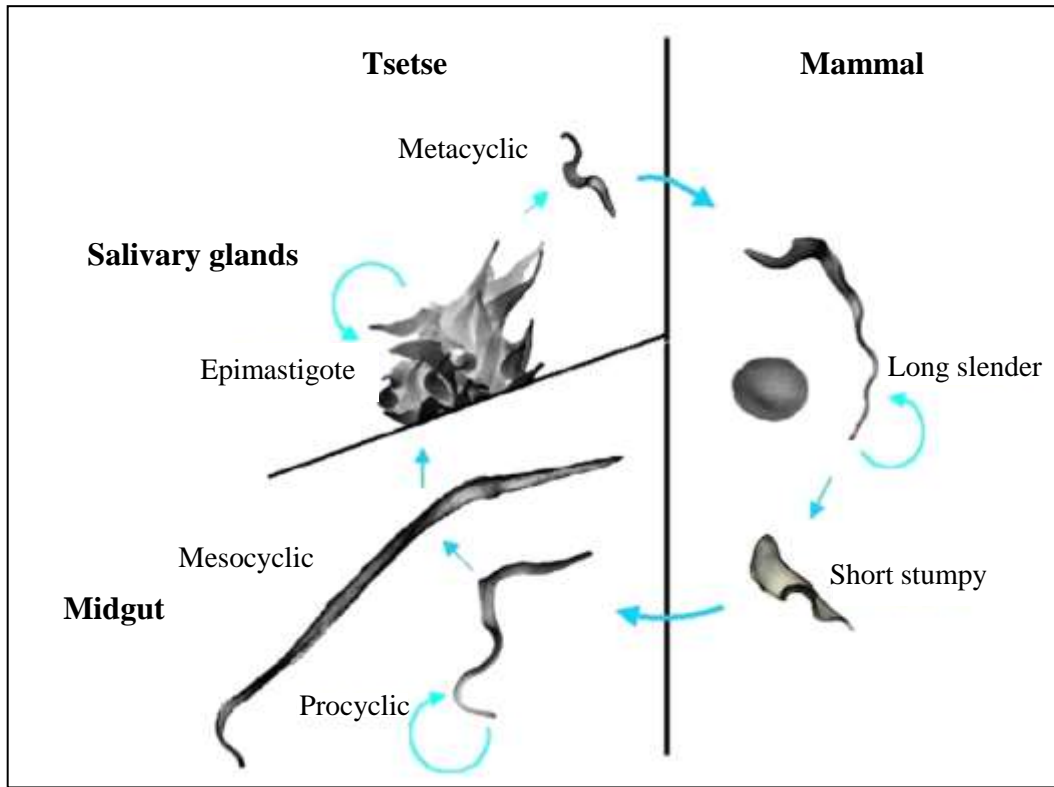


Figure 2.2: Life cycle of *T. brucei*. Adapted from Holmes (2003).

## 2.2 Human African trypanosomiasis

The vector-borne parasitic disease, Human African Trypanosomiasis (HAT) or most commonly known as sleeping sickness is caused by two sub-species of protozoan haemoflagellates *T. brucei* i.e., *T. b. gambiense* and *T. b. rhodesiense*. HAT is transmitted to humans by the bite of a tsetse fly (genus *Glossina*). Sleeping sickness is restricted to sub-Saharan Africa where the insect vector resides. HAT is recognized as the most Neglected Tropical Disease (NTD) by World Health Organization (WHO). The NTD is a group of tropical infections that trouble more than 1 billion poor populations of 149 developing countries in Asia, Americas, and sub-Saharan Africa. In addition, they contribute a worldwide disease burden equivalent to the group of HIV/AIDS with an estimated up to 1 million deaths every year (Zahari *et al.*, 2014). In 2000, it was estimated only 0.1% of worldwide funding was allocated to drug discovery for tuberculosis and selected tropical diseases (e.g., malaria, trypanosomiasis and leishmaniasis), which together account for about 5% of the global disease burden (Pink *et al.*, 2005).

The distribution of HAT throughout 36 countries in sub-Saharan African covering an area of 10 million km<sup>2</sup> between 14° North and 20° South latitude and about 50 million people are at risk from the disease (Keating *et al.*, 2015; Bacchi, 2009; Steverding, 2008; Kennedy, 2006). Figure 2.3 shows the distribution of HAT with incidences and risk for travelers. In the early of 19<sup>th</sup> century, epidemics of HAT were reported after major outbreaks. Chemotherapy, vector control and disease surveillance have been set up to combat the disease. With less than 5,000 cases reported in the entire continent, the disease was almost eliminated in the mid-1960s (Franco *et al.*, 2014; Brun *et al.*, 2010). However, the disease resurged in the late 1990s. In 2006, approximately 50,000 to 70,000 new cases reported in Africa each

year, with annual incidence of HAT was estimated as 17,500 new cases (Sykes and Avery, 2009a; Sykes and Avery, 2009b). Although the number of reported cases in 1998 decreased from 37,385 to 3,796 in 2014, which is likely to represent only a small number of the true cases being reported, many remain unreported and thus untreated, owing to the limited access to the isolated regions and lack of health provision (Jones and Avery, 2015; Faria *et al.*, 2014). The disease affects mainly poor nations and communities living in remote countryside areas of Africa. People also risk becoming infected if they travel through countries where the insect vector is prevalent.

*T. b. gambiense* is responsible for a chronic infection, widespread in 24 countries in west and central Africa, contributes for more than 95% of reported cases of sleeping sickness (Reet *et al.*, 2013). A person can be infected for up to a year or more without major signs and symptoms of the disease. When more obvious symptoms appear, the patient is usually in a late stage of the disease where the CNS is affected (Ioset *et al.*, 2009). In contrast to *T. b. gambiense*, *T. b. rhodesiense* causes an acute infection, common in 13 countries in eastern and southern Africa (Barrett *et al.*, 2007). Nowadays, this form accounts for less than 5% of reported cases (Faria *et al.*, 2014). First signs and symptoms are observed a few weeks or months after infection. The disease develops rapidly and invades the CNS (Ioset *et al.*, 2009). Ultimately, without treatment, HAT is fatal. There is another form of trypanosomiasis which is caused by *Trypanosoma cruzi* and transmitted by triatomine bug. The disease is known as American trypanosomiasis or Chagas disease happens mainly in Latin America (Njiru *et al.*, 2004; Barrett *et al.*, 2003).

Sleeping sickness has two distinct stages. The early stage or haemolymphatic phase, the trypanosomes multiply in the blood and lymphatic system. The symptoms of this



stage are itching, fever, headaches, and joints pain (Sykes and Avery, 2009b). In the late stage or neurological phase, the trypanosomes crossed the BBB into the spinal fluid, infesting the CNS including the brain, causes severe neurologic symptoms and changes in behavior, confusion, poor coordination, difficulties with speech, and finally disturbance of sleep (somnolescent state), giving the disease its name (Sykes and Avery, 2009a). Without treatment of the infection, the patients die within years when infected with *T. b. gambiense* or within months when infected with *T. b. rhodesiense* (Steverding, 2008).

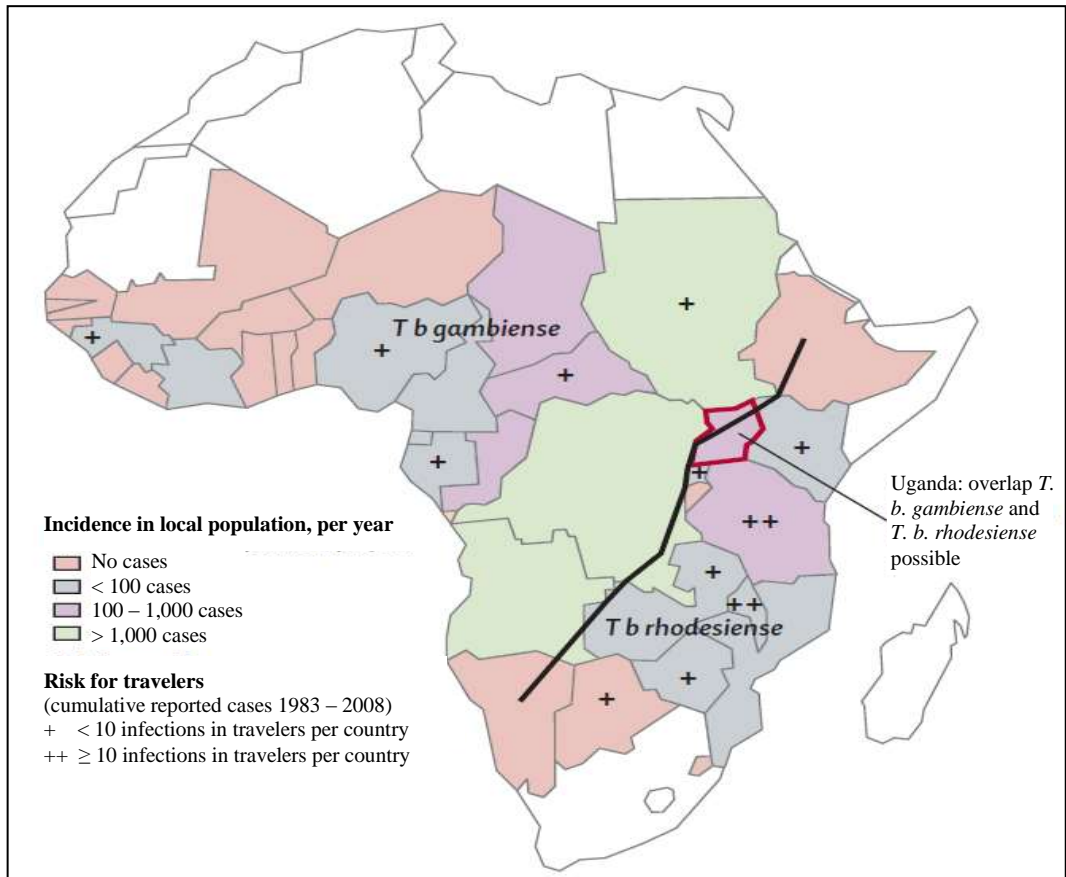


Figure 2.3: Distribution of HAT with incidences and risk for travelers. Adapted from Brun (2010).

### 2.2.1 Diagnosis of HAT

To avoid the disease from progressing to the second stage, diagnosis must be made as early as possible. Early screening for possible infection involves checking for clinical signs (swollen cervical lymph nodes) and neurological signs (extended daytime sleeping), or using serological tests such as card agglutination trypanosomiasis test (CATT) (Truc *et al.*, 2002). Nevertheless, CATT is only available for examining *T. b. gambiense* infection and is not applicable to *rhodesiense* forms. Diagnosis is easily achieved by microscopic examination of the peripheral blood smear in the acute form of the disease caused by *T. b. rhodesiense* (Kennedy, 2006). However, small parasitemia levels can make it difficult to see the parasites microscopically. If the parasites have crossed the BBB to initiate neurological stage, examining the sample of cerebrospinal fluid via a lumbar puncture is required. In the recent development of the new diagnostic methods for HAT, much effort has been made in the improvement of the molecular tools to overcome the existing limitations of serological and parasitologic diagnostic methods (Simarro *et al.*, 2008). Detection of parasites nucleic acids by PCR-based detection of infection from the unique genes for both *T. b. gambiense* (TgsGP gene) and *T. b. rhodesiense* (SRA gene) (Radwanska *et al.*, 2002a; Radwanska *et al.*, 2002b; Welburn *et al.*, 2001), molecular dipstick tests allow easier reading of the PCR results (Deborggraeve *et al.*, 2006), and the loop-mediated isothermal amplification, which is highly sensitive, specific and easy diagnostic assay for the detection of parasites in the *T. brucei* group (Kuboki *et al.*, 2003) become useful as a more sensitive approach.

### 2.2.2 Treatment of HAT

As developing effective drugs requires high costs and resources, most pharmaceutical companies are unwilling to develop drugs for this disease (Martyn *et al.*, 2007). Drugs are the only main control strategy for HAT because there are no vaccines available in the market. However, HAT chemotherapy relies upon a limited number of drugs, have associated toxicity effects or impractical administration regimes (Sykes and Avery, 2009b). The drugs for treating sleeping sickness are depending on the causative subspecies and stage of the disease. In general, if the disease is identified earlier, it is curable if treatment is given quickly. The drugs used in the HAT treatment of early stage generally safer and easier to administer, usually requires several injections. Treatment becomes much more violent when the parasites have crossed the BBB. Toxic arsenic drug such as melarsoprol is used to kill the parasites. Drugs used in treating late stage of HAT have complex regimen and difficult to apply, normally in the form of a series of intravenous infusions for few weeks. In addition, the assessment of post-treatment requires follow up of the patient for up to 2 years and involves laboratory tests of cerebrospinal fluid obtained through lumbar puncture because the parasites may stay viable and reproduce the disease months after treatment.

Currently there are few drugs approved for the treatment of HAT such as pentamidine, suramin, melarsoprol, and eflornithine (Figure 2.4). Table 2.1 summarizes the drug therapy in HAT. The drugs are distributed free of charge to disease prevalent countries. The other drugs were discovered before 1950s except for eflornithine (Phillips *et al.*, 2013; Steverding, 2010). Main issues with drug treatment include poor efficacy, adverse side-effect and the chemotherapy treatment is complicated. First stage of disease is only treatable with suramin and pentamidine,

whereas melarsoprol (useful against *T. b. rhodesiense* and *T. b. gambiense*) and eflornithine (only active against *T. b. gambiense*) are only effective against the second stage of disease. Melarsoprol is an arsenic derivative and toxic to be used because it causes reactive encephalopathy in up to 10% of treated patients, in which half of these patients die from this harmful reaction (Bowling *et al.*, 2012). It is currently used as front-line treatment for the *rhodesiense* form, and as alternative therapy for the *gambiense* form. Meanwhile, there has also been a spread of resistance to melarsoprol in trypanosomes found in central Africa (Abdel-Sattar *et al.*, 2008). There are also increasing reports of treatment failures, particularly with melarsoprol (Hoet *et al.*, 2004). Although eflornithine is safer than melarsoprol however, it needs several intravenous infusions per day, which needs extra costs.

In addition, the development of vaccine for the treatment of the disease is difficult because of the antigenic variation that protects the parasite to survive attack by the host's immune system (Bacchi, 2009). Furthermore, the mechanisms of action of these drugs still uncertain except for eflornithine, which selectively inhibits polyamine biosynthesis pathway (ornithine decarboxylase) in the parasite (Barrett *et al.*, 2011). A drug registered for the treatment of Chagas disease i.e., Nifurtimox was introduced in 2009 in the WHO's List of Essential Medicines (Faria *et al.*, 2014), and is currently suggested as front-line treatment for the *gambiense* form after efficacy and safety statistics provided by clinical trials. The nifurtimox-eflornithine combination therapy (NECT) is being used as an alternative therapy for melarsoprol-refractory late stage disease (Barrett *et al.*, 2007). The NECT reduces the number of intravenous perfusions with eflornithine and the time of treatment (Jones *et al.*, 2013). However, NECT has not been studied for *T. b. rhodesiense* and thus not applicable to *rhodesiense* form.

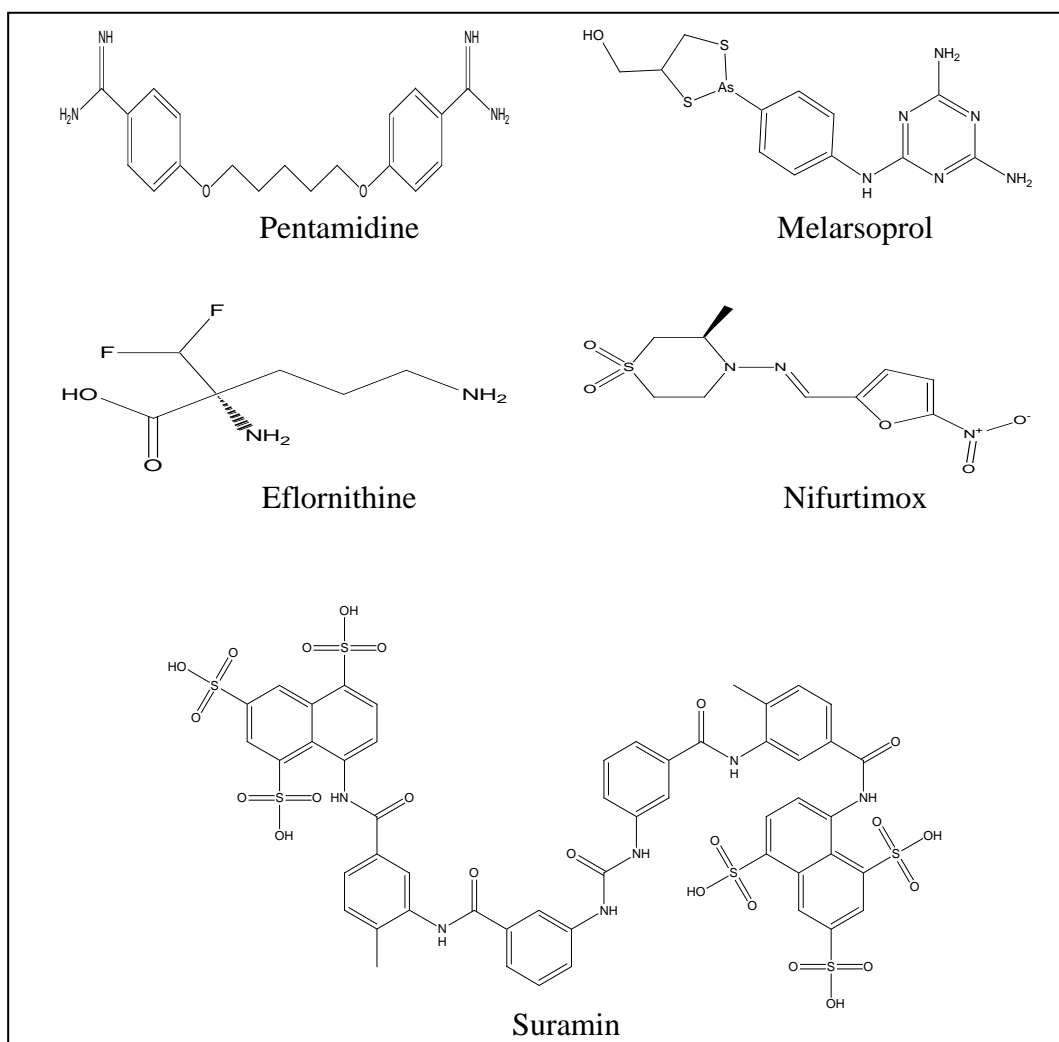


Figure 2.4: Chemical structure of registered drugs used in the treatment of HAT.

Table 2.1: Summary of drug therapy in HAT.

Disease	Front-line therapy	Alternative therapy
Early stage of <i>T. b. gambiense</i>	Pentamidine	Suramin
Early stage of <i>T. b. rhodesiense</i>	Suramin	None
Late stage of <i>T. b. gambiense</i>	Eflornithine	Nifurtimox- eflornithine
Late stage of <i>T. b. rhodesiense</i>	Melarsoprol	None

### 2.3 High-throughput screening in anti-trypanosomal drug discovery

Whole cell *in vitro* HTS is a well-established approach for drug discovery programs in neglected disease area for some times and is now in use to search for new trypanocidal candidates against large compound libraries. In addition, whole cell-based assays have been successful in resulting in development of drugs for parasitic disease in general (Pink *et al.*, 2005). Hence, HTS is a main consideration for HAT drug discovery programs. Initially the assays were carried out in 96-well plates but with the current technology advancement there are also 1,536-well plates available. Typical HTS programs can perform 10,000 assays in a day, while some laboratories with ultra high-throughput screening (UHTS) have potential to screen up to 100,000 compounds per day. The whole cell based screening assays are highly physiologically relevant because whole cells instead of a specific target are used as screening models. In addition, the whole cell based assay only need a simple pathogen viability readout (Faria *et al.*, 2014). Therefore, this approach has the potential of identifying new leads and drug targets with novel modes of action.

For determination of trypanosomes cellular viability, few assay formats have been adopted to screen *T. brucei* sp. via counting  $^3\text{H}$ -hypoxanthine incorporation, nuclear staining techniques, flow cytometry, and measurement of culture pH (Sykes and Avery, 2009b; Kaminsky and Brun, 1993). The resazurin-based assay or most commonly known as Alamar Blue™ (commercially available solution) assay is very cost-effective and is a good non-radioactive alternative to the other conventional assay. Resazurin was initially used in 1950s to measure the viability of sperm and to evaluate contaminants in biological fluids and milk by colorimetry (ÓBrien *et al.*, 2000). A viability assay in 96-well format, which utilizes the dye Alamar Blue™, has been widely reported in the literature for *T. brucei* sp. (Merschjohann and Steverding,

2006; Raz *et al.*, 1997). It has been shown to have great potential for the determination of drug sensitivities of African trypanosomes *in vitro* because it is non-toxic to trypanosomes (Raz *et al.*, 1997). Resazurin-based assay involves only a single step of preparation. Cell lysis, washing or extraction procedures normally are not required (Mackey *et al.*, 2006; Onyango *et al.*, 2000; Raz *et al.*, 1997). The cell viability assay by resazurin is based on the principle of reduction of the non-fluorescent reagent (resazurin) to a fluorescent compound (resorufin) by the intracellular reducing environment of living cells over time (Munshi *et al.*, 2014). It has been proposed that the reduction of resazurin are part of the glycolytic pathway in bloodstream trypanosomes because they rely on glycolytic pathway for energy production (Raz *et al.*, 1997).

In general, after 72 h treatment with compounds, the cell viability of bloodstream form trypanosomes from *in vitro* or *in vivo* cultures is evaluated using either colorimetric, radioactive, fluorometric, or luminescent detection. For example, viability assays based on ATP-reduction such as luciferase- and resazurin-based whole cell viability assays have been used extensively in 96- and 384-well format for high-throughput compound screening of *T. brucei* spp. owing to their sensitive, easy and quick readout (Sykes and Avery, 2009a; Sykes and Avery, 2009b; Mackey *et al.*, 2006). The latter was used to screen 87,296 compounds against *T. b. brucei* bloodstream form strain 427 in 384-well format with 205 compounds showed greater activity. Further testing against *T. b. rhodesiense* in 96-well format resulting in 6 hits from 5 new chemical classes with anti-proliferative activity confirmed (Sykes *et al.*, 2012).



### 2.3.1 HTS assays formats: 96-, 384- and 1536-well formats

For many years, HTS assays have been carried out in the typical 96-well microplate. The recent objective of most companies is to surpass this format to lower volume and higher density formats (e.g., 384- and 1536-well microplates). The advantages of using 384- and 1536-well microplates are increased throughput and lower volume, which requires lower cost. Rather than increase in throughput, cost-effective is the main reason for many HTS researchers to move to 384- and 1536-well microplates. The common features of a 96-well plate consist of column 1 – 12 (12 columns) and row A – H (8 rows). In comparison with 384- and 1536-well formats, each individual well of the 96-well plate contain 4- and 16-subwells in 384- and 1536-well plate, respectively. Hence, these plates are subdivided into column 1 – 24 (24 columns) and row A – P (16 rows) in a 384-well plate, and column 1 – 48 (48 columns) and row A – Z and A – F (32 rows) in a 1536-well plate. With reference to the 96-well plate, the 384-well plate has four quadrants (1A, 2A, 1B, 2B), whereas the 1536-well plate has sixteen quadrants i.e., 1A – 4A, 1B – 4B, 1C – 4C, 1D – 4D corresponding to well 1A of the 96-well plate (Figure 2.5). When the 96-channel pipetting head of the liquid handler interacts with different plate formats, one stroke is needed within a 96-well plate. In contrast to the 96-well plate, four strokes are needed when a 384-well plate is used, each one corresponding to one of four quadrants. Furthermore, when a 1536-well plate is used, sixteen strokes are needed. Therefore, four full 96-well plates is needed to fill an empty 384-well plate and sixteen full 96-well plates is required to occupied one whole 1536-well plate. In order to restore the actual replicates in the wells of the different plate formats compared to 96-well format, samples in at least four wells in 384-well plate and sixteen wells in 1536-well plate have to be harvested and counted (Pira *et al.*, 2012).